Ultra Wide Band Wireless Communications : A Tutorial

Maria-Gabriella Di Benedetto and Branimir R. Vojcic

Abstract: **Ultra wide band (UWB) radio has recently attracted increased attention due to its expected unlicensed operation, and potential to provide very high data rates at relatively short ranges. In this article we briefly describe some main candidate multiple access and modulation schemes for UWB communications, followed with their power spectral density calculation and properties. We also present some illustrative capacity results, and provide a discussion of the impact of network topology on multiple access capacity.**

Index Terms: **Ultra wide band communications, spread spectrum, direct sequence, time hopping, code division multiple access, ad-hoc networks.**

I. INTRODUCTION

Ultra wide band (UWB) radio is based on the radiation of waveforms formed by a sequence of very short pulses; very short refers to pulse duration which in communication applications is typically of about a few hundreds of picoseconds. The information to be transferred is usually represented in digital form by a binary sequence, and each bit is transferred using one or more pulses.

The most common adoption of the term Ultra Wide Band comes from the radar world and refers to electromagnetic waveforms which are characterized by an instantaneous fractional energy bandwidth greater than about 0.20–0.25. The energy bandwidth is identified by two frequencies f_L and f_H which delimit the interval where most of the energy of the waveform E (say over 90%) falls. We call energy bandwidth the width of the interval $[f_L, f_H]$, i.e., $f_H - f_L$. Note that E must be computed over an interval which corresponds to the set of pulses involved in the decision of a single bit.

In a recent release of UWB devices emission masks in the United States of America (FCC, 2002) f_L and f_H have been set to the lower and upper frequencies of the -10 dB emission points. The selection of the -10 dB over the -20 dB bandwidth, as established by the Defence Advanced Research Projects Agency (DARPA, 1990), is motivated by the recommended restriction of UWB emissions to very low power levels, i.e., below -41.3 dBm/MHz, i.e., close to the noise floor. Under these conditions, the -20 dB emission points cannot be measured reliably. The same release (FCC, 2002) specifies that a signal is UWB if its bandwidth at -10 dB points exceeds 500 MHz, regardless of the fractional bandwidth value. The 500 MHz value is lower than the 1.5GHz minimum bandwidth established by DARPA (DARPA, 1990), as motivated by the use of a -10 dB over the -20 dB bandwidth. The 500 MHz minimum bandwidth sets a threshold at 2.5GHz below which signals are UWB if their bandwidth exceeds 500 MHz. Above threshold, signals are UWB if their fractional bandwidth exceeds 0.2.

The above definitions comply with the traditional radio communication concept that a signal is wideband or broadband (vs. narrowband) when its bandwidth is large (vs. small) with respect to the modulating carrier frequency. In the case of UWB, due to the absence in general of a modulating carrier frequency, reference is made to the center frequency of spectrum occupation.

It is intuitive to predict that signals formed by pulses with duration in the order of fractions of nanoseconds will very likely be UWB. While in radars in fact there are arguments which favor pulse lengthening, when it comes to communication applications the shorter the pulse the better, since the resource, which is time here, is better exploited. Note though that the signal used for transmission consists of a sequence of these pulses, which are modulated by the information data symbols. It remains therefore to derive the power spectral density (PSD) and related bandwidth of the multi-pulse signal. This analysis is reported in Section II which contains a review of UWB radio principles. In particular we will illustrate how the characteristics of a single pulse impact the spectrum of the UWB signal. In Section III we will address power limitations, and how to shape the PSD by modifying the pulse waveform. Section IV deals with different aspects of multiple access technology, including the theoretical capacity, comparison of time-hopping and direct-sequence code division multiple access and topological considerations.

II. REVIEW OF ULTRA WIDE BAND RADIO PRINCIPLES

As previously mentioned the most common and traditional way of emitting an UWB signal is by radiating pulses which are very short in time. The way by which the information data symbols modulate the pulses may vary; pulse position modulation (PPM) and pulse amplitude modulation (PAM) are often considered modulation schemes[1] [Welborn, 2001; Guvenc and Arslan, 2003]. In addition to modulation, and in order to shape the spectrum of the generated signal, the data symbols are encoded using pseudorandom or pseudo-noise (PN) sequences. In a common approach the encoded data symbols introduce a time dither on generated pulses leading to the so-called time-hopping UWB (TH-UWB). Direct-sequence spread spectrum (DS-SS), i.e., amplitude modulation of basic pulses by encoded data symbols in its impulse radio version, indicated as DS-UWB, also seems particularly attractive (Huang and Li, 2001; Foerster J.R. 2002; Vojcic and Pickholtz, 2003). As well known DS-SS has

Manuscript received November 25, 2003.

M.-G. Di Benedetto is with the University of Rome La Sapienza, College of Engineering, Infocom Department, Via Eudossiana, 18-00184 Rome, Italy, email: dibenedetto@newyork.ing.uniroma1.it.

B. R. Vojcic is with the George Washington University, Department of Electrical and Computer Engineering, 801 22nd Street, NW, Washington DC 20052, USA, email: vojcic@gwu.edu.

[1] To our knowledge there is no proposed system making use of pulse duration modulation (PDM).

1229-2370/03/$10.00

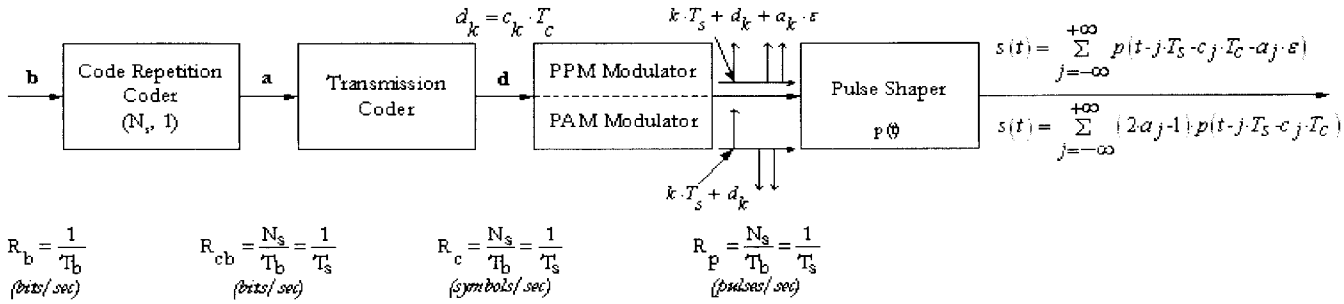

Fig. 1. Transmission scheme for a TH-UWB signal.

been adopted as the basic radio-access technology for third generation wireless communication systems (in Europe, Japan and USA, as well as many other countries), and applying consolidated concepts is definitely appealing.

The UWB definition released by the FCC as mentioned in the Introduction (FCC, 2002) does not limit the generation of UWB signals to impulse radio, and opens the way at least in the USA for alternative, i.e., non-impulsive schemes. An ultra wide bandwidth, say 500 MHz, might be produced by a very high data rate, independently of the characteristics of the pulses. The pulses might for example satisfy the Nyquist criterion at operating pulse rate $1/T$, which would require a minimum bandwidth of $B = 1/2T$, and thus be limited in frequency but unlimited in time having the classical raised-cosine infinity-bouncing shape with nulls at multiples of $1/T$. Systems with an ultra wide bandwidth of emission due to high speed data rate rather than pulse width, provided that the fractional bandwidth or minimum bandwidth requirements are verified at all times of the transmission, are not precluded. Methods such as for example orthogonal frequency division multiplexing (OFDM) and multi-carrier code division multiple access (MC-CDMA) are capable of generating UWB signals, at appropriate data rates. Recent proposals in the USA, and in particular in the IEEE 802.15-3a working group, refer to a multi-band alternative in which the overall available bandwidth is divided into subbands of at least 500 MHz (Foerster *et al.*, 2003; Yeh *et al.*, 2003). Frequency-hopping spread spectrum (FH-SS) might also be a viable way. This approach is currently less in vogue due to the difficulty in measuring the bandwidth at all instants of time, i.e., stopping the frequency sweep, and therefore complying with minimum bandwidth requirements. All of these methods are well-known in the wireless communications community, and are generously described in scientific journals and books (Proakis and Salehi, 1994; Webb and Hanzo, 1995). A detailed analysis of all of these methods which would represent a mere duplication of a well-consolidated literature is definitely out of the scope of this paper. Focus will be on impulse radio UWB and specifically TH-UWB and DS-UWB in which spectrum expansion is obtained by using very short pulses besides the spreading introduced by coding. RF modulation is rarely mentioned in UWB systems which typically operate in the baseband. While RF modulation is obviously applicable to UWB as well, a shift in operating frequency can be potentially obtained here by pulse shaping.

Since modulation and multiple access are independent processes, TH-UWB and DS-UWB may adopt in principle, either PPM or PAM for data modulation. A specific modulation scheme might be more appropriate for one or the other scheme, as a function of the resulting spectrum shape and characteristics.

We now focus on the generation process for TH-UWB and DS-UWB signals, and on derivation of related power spectral densities (PSDs).

A. *Generation of Time-Hopping UWB and Direct-Sequence UWB Signals*

Fig. 1 shows the general transmission scheme for a TH-UWB signal. A channel coder, which is in particular a $(N_s, 1)$ block code-repetition coder, introduces redundancy by repeating N_s times each bit of the source **b** sequence, and generates a binary sequence **a** at rate R_{cb}=N_s/T_b=$1/T_s$ bits/sec, where $R_b = 1/T_b$ is the bit rate of the source. A transmission coder applies then an integer-valued code **c**= $(\cdots, c_0, c_1, \cdots, c_k, c_{k+1}, \cdots)$, which is usually periodic with period N_p, to **a**, and produces a sequence **d**. The **d** sequence elements are $d_j = c_j T_c$, with $c_j T_c < T_s$ for all c_j. We assume for now that **c** is a pseudo-random code, its generic element c_j being an integer verifying $0 \leq c_j \leq N_h$. Analysis of different transmission codes can be found for example in [Iacobucci and DiBenedetto, 2002; Laney *et al.*, 2002]. The effect of the transmission coder is to shape the spectrum of the transmitted signal. In a multi-user environment it plays in addition the role of code-division coder, with different users being assigned with different codes. Sequence **d** enters the modulator which generates a sequence of Dirac pulses $\delta(t)$ at a rate $R_p = N_s/T_b = 1/T_s$ pulses/sec. These pulses are located at times $kT_s + d_k T_c$, and are therefore shifted in time from nominal positions kT_s by $d_k T_c$. Note that the effect of the **c** code is to introduce time-hopping (TH) on generated pulses. According to the information bit value, the pulses are then either position modulated (pulse position modulation, PPM) or amplitude modulated (pulse amplitude modulation, PAM) with binary antipodal modulation (BAM) as a subcase. In the case of PPM pulses corresponding to a 1-bit are shifted by a small quantity ϵ while the position of the 0-bit pulses is kept unchanged. In PAM the amplitude of the pulse remains unchanged for a 1-bit, while a 0-bit inverts pulse polarity. Finally the last system is the Pulse Shaper filter with impulse response $p(t)$. The impulse response $p(t)$ must be such that the generated signal is a sequence of strictly non-overlapping pulses.

The signal $s(t)$ at the output of the cascade of the above systems in the case of PPM is:

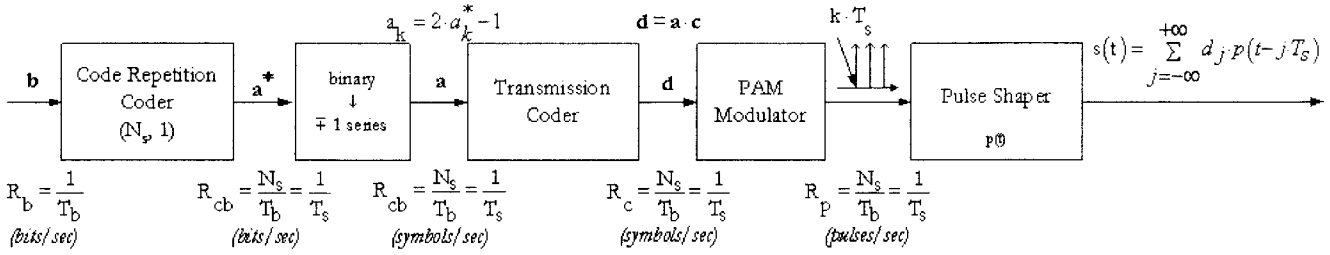

Fig. 2. Transmission scheme for a DS-UWB signal.

$$s(t) = \sum_{j=-\infty}^{+\infty} p(t - jT_s - c_jT_c - \epsilon \cdot a_j) = \sum_{j=-\infty}^{+\infty} p(t - jT_s - \eta_j - \epsilon \cdot a_j). \quad (1)$$

The bit interval, or bit duration, i.e., the time used to transmit one bit, T_b, is: $T_b = N_sT_s$. The term c_jT_c defines pulse randomization or dithering with respect to nominal instants of time occurring at multiples of T_s and is represented by a random time-hopping dither η_j which can be assumed to be uniformly distributed between 0 and $T_\eta < T_s$. Note that η_j is usually much larger than ϵ. The joint effect of ϵ and η_j is to introduce a random time-shift distributed between 0 and $T + \epsilon < T_s$ indicated by θ_j, i.e.:

$$s(t) = \sum_{j=-\infty}^{+\infty} p(t - jT_s - \theta_j). \quad (2)$$

The concept leading to (2) can be generalized, the idea being of transmitting two different pulse shapes $p_0(t)$ and $p_1(t)$ corresponding to the information bits "0" and "1", respectively. Note that the above analyzed case of a PPM modulator which introduces a time-shift ϵdepending on the bit value is a particular case in which $p_1(t)$ is a shifted version of $p_0(t)$. A more general expression is:

$$s(t) = \sum_{j=-\infty}^{+\infty} p_{a_j}(t - jT_s - c_jT_c) = \sum_{j=-\infty}^{+\infty} p_{a_j}(t - jT_s - \eta_j), \quad (3)$$

which also represents the case of TH-UWB in combination with BAM when $p_1(t)$ is set to be $-p_0(t)$.

UWB signals can also be generated in a Direct-Sequence Spread-Spectrum fashion by first coding the binary sequence to be transmitted with a PN binary-valued sequence, and then by amplitude modulating a train of short pulses. This operation can be seen as a version of currently in use DS-SS systems in which pulses are usually of the Nyquist type of rate $1/T_c$ indicated as chip rate.

The resulting DS-UWB signal can be generated as shown in Fig. 2 Given the binary source sequence **b** at a rate $R_b = 1/T_b$ bits/sec, an $(N_s, 1)$ code-repetition coder repeats each bit N_s times and generates a binary sequence **a** at rate $R_{cb} = N_s/T_b = 1/T_s$ bits/sec. A second system transforms the **a** sequence into a positive and negative valued sequence **a**= $(\cdots, a_0, a_1, \cdots, a_k, a_{k+1}, \cdots)$, i.e., $(a_k = 2b_k - 1, -\infty < k < +\infty)$. The transmission coder applies then a binary code **c**= $(\cdots, c_0, c_1, \cdots, c_k, c_{k+1}, \cdots)$, composed of ± 1's and of period N_p, to the sequence **a**= $(\cdots, a_0, a_1, \cdots, a_k, a_{k+1}, \cdots)$, and generates a new sequence **d=ac**. N_p is commonly assumed to be equal to N_s, or as a multiple of N_s. Note that **d** is a ± 1's sequence as is **a** and is generated at a rate $R_{cb} = N_s/T_b = 1/T_s$ bits/sec. The sequence **d** enters the BAM modulator which produces Dirac pulses $\delta(t)$ at rate $R_p = N_s/T_b = 1/T_s$ pulses/sec located at kT_s. Finally the signal is shaped by the pulse shaping filter of impulse response $p(t)$.

The resulting signal $s(t)$ can be expressed as follows:

$$s(t) = \sum_{j=-\infty}^{+\infty} p(t - jT_s). \quad (4)$$

Note that as in the TH case the bit rate is $1/T_b = 1/N_sT_s$.

The resulting waveform is a straightforward PAM waveform. One can expect that evaluating the PSD of the signal of (4) is simpler than for (2), given the occurrence of pulses at regular time intervals.

B. Power Spectral Density of PPM Time-Hopping UWB Signals

B.1 Borrowing from the past: Analog PPM

Equation (2) has strong similarities with the output of a analog PPM modulator consisting of a train of identically shaped and strictly non-overlapping pulses which are shifted from multiples of T_s by the samples $m(kT_s)$ of a modulating signal $m(t)$:

$$x_{PPM}(t) = \sum_{j=-\infty}^{+\infty} p(t - jT_s - m(jT_s)) = p(t) * \sum_{j=-\infty}^{+\infty} \delta(t - jT_s - m(jT_s)). \quad (5)$$

The spectrum of a PPM signal is difficult to evaluate due to the non-linear nature of PPM modulation. The complete derivation of this spectrum can be found in (Rowe, 1964), and is based on various articles by Bennett published from 1933 to 1947 (Bennett, 1933; Bennett, 1944; Bennett, 1947). We will report here

only the principal results for three particular cases which are of interest in understanding the spectrum of a PPM-TH-UWB signal, i.e., a) sinusoidal modulating signals; b) generic periodic modulating signals; c) randomly modulated signals.

a) Sinusoidal modulating signals

Consider a modulating signal at frequency $f_0 << 1/T_s$. One has then:

$$x_{PPM}(t) = p(t) * \sum_{j=-\infty}^{+\infty} \delta(t - jT_s - Acos2\pi f_0 jT_s). \quad (6)$$

If $P(f) = \int_{-\infty}^{\infty} p(t)e^{j2\pi ft}dt$ indicates the Fourier transform of $p(t)$, an expansion of $x_{PPM}(t)$ into sinusoidal components can be found which writes:

$$x_{PPM}(t)=\frac{1}{T_s}\sum_{m=-\infty}^{+\infty}\sum_{n=-\infty}^{+\infty}(-j)^n J_n\left(2\pi A(m\frac{1}{T_s}+nf_0)\right) \cdot P\left(m\frac{1}{T_s}+nf_0\right)e^{j2\pi(m\frac{1}{T_s}+nf_0)t}, \quad (7)$$

where J_n is the Bessel functions of the first kind and the n-th order. Properties and curves for the Bessel functions can be found in many communication systems books since these functions appear in the computation of the spectrum of angle modulated signals (see for example Proakis and Salehi, 1994). From (7) the PSD of $x_{PPM}(t)$ is thus:

$$\mathbf{P}_{x_{PPM}}(f) = \frac{1}{T_s^2}\sum_{m=-\infty}^{+\infty}\sum_{n=-\infty}^{+\infty}\left|J_n\left(2\pi A(m\frac{1}{T_s}+nf_0)\right)\right|^2 \cdot\left|P\left(m\frac{1}{T_s}+nf_0\right)\right|^2\cdot\delta\left(f-(m\frac{1}{T_s}+nf_0)\right). \quad (8)$$

Equation (8) shows that when $m(t)$ is a sinusoidal waveform, the PPM signal contains discrete frequency components located at the sinewave frequency f_0 and pulse repetition frequency $1/T_s$ and harmonics, and at the sum and difference of f_0 and $1/T_s$ and harmonics. The amplitude is governed by two terms, $P(f)$ and $J_n(x)$. If $P(f)$ has limited bandwidth, the bandwidth of the PPM signal is limited as well. Regarding $J_n(x)$, let us first observe that for $n = 0$, $J_n(x) = 1$ if $x = 0$. Since from (8) $x = 2\pi A_m/T_s$ for $n = 0$, one has $x = 0$ when $m = 0$. Recall that since m is the index referring to the harmonics of $1/T_s$, for all $m \neq 0$, the discrete frequency components at frequencies m/T_s are present with amplitude given by $|J_n(2\pi A_m/T_s)|^2$. Since m spans the infinite interval of summation the term $J_n(x)$ does not introduce a limitation in the bandwidth of the signal of (8). It does regulate the presence vs. absence of pulses located at multiples of f_0 and of linear combinations of f_0 and $1/T_s$.

b) Periodic modulating signals

When $m(t)$ has period T_p, i.e., $m(t+T_p) = m(t)$, for all t, the Fourier series representation of $m(t)$ is valid for all t. By applying the multiple Fourier series method as proposed by Bennett (1933, 1944, and 1947) and further suggested by Rowe (1965) one finds:

$$x_{PPM}=\frac{1}{T_s}\sum_{m=-\infty}^{+\infty}\sum_{n=-\infty}^{+\infty}\sum_{l=-\infty}^{+\infty}(-j)^n J_n\left(2\pi M\left(m\frac{1}{T_s}+nl\frac{1}{T_p}\right)\right) \cdot P\left(m\frac{1}{T_s}+nl\frac{1}{T_p}\right)e^{j2\pi(m\frac{1}{T_s}+nl\frac{1}{T_p})t}. \quad (9)$$

(9) easily leads to the PSD of a periodic modulating PPM signal $x_{PPM}(t)$, i.e.,:

$$\mathbf{P}_{x_{PPM}}(f) = \frac{1}{T_s^2}\sum_{m=-\infty}^{+\infty}\sum_{n=-\infty}^{+\infty}\sum_{l=-\infty}^{+\infty}\left|J_n\left(2\pi M(m\frac{1}{T_s}+nl\frac{1}{T_p})\right)\right|^2 \cdot\left|P\left(m\frac{1}{T_s}+nl\frac{1}{T_p}\right)\right|^2\cdot\delta\left(f-(m\frac{1}{T_s}+nl\frac{1}{T_p})\right). \quad (10)$$

Similarly to the sinusoidal case, when the modulating signal is a periodic waveform, the PPM signal contains discrete frequency components located at the fundamental and pulse repetition frequencies and harmonics, and at the sum and difference of fundamental and pulse repetition frequencies and harmonics. The amplitude is governed by the two terms, $P(f)$ and $J_n(x)$ and closely follows the sinusoidal case.

c) Randomly modulating signals

The derivation of the PSD of (5) can be carried out under the hypotheses that: 1) $m(kT_s)$ is a stationary discrete random process, where $m(kT_s)$ are the samples of a stationary continuous process $m(t)$, and that: 2) the different $m(kT_s)$ are statistically independent with a common probability density function $w(m(kT_s))$.

Since the signal of (5) is not wide-sense stationary, the PSD for this signal $\mathbf{P}_{x_{PPM}}(f)$ must be found by first computing the autocorrelation function of a particular $x_{PPM}(t)$, averaging over the ensemble to find the ensemble average, and finally obtain $\mathbf{P}_{x_{PPM}}(f)$ by taking the Fourier transform of the ensemble average. One obtains:

$$\mathbf{P}_{x_{PPM}}(f) = \frac{|P(f)|^2}{T_s}\left[1-|W(f)|^2+\frac{|W(f)|^2}{T_s}\sum_{n=-\infty}^{+\infty}\delta(f-\frac{n}{T_s})\right], \quad (11)$$

where $W(f)$ is the Fourier transform of the probability density w, and coincides with the characteristic function of w computed in $-2\pi f$:

$$W(f) = \int_{-\infty}^{+\infty} w(s)e^{-j2\pi fs}ds = \left\langle e^{-j2\pi fs}\right\rangle = C(-2\pi f). \quad (12)$$

Equation (11) shows that the spectrum of a randomly modulating PPM signal is composed of a continuous part controlled by the term $1-|W(f)|^2$, and of a discrete part formed by line components at multiples of $1/T_s$. The discrete part corresponds to a periodic component in the PPM signal of (5).

Since $W(f)$ is the Fourier transform of a probability density function, $W(0) = 1$ and therefore the continuous component of the spectrum is zero at frequency zero, and therefore necessarily rises at higher frequencies. The discrete components which are weighted by $|W(f)|^2$ are larger at low frequencies then decrease at high frequencies. The predominance of the continuous term over the discrete term depends upon the values of $m(kT_s)$. If these are small then the PPM signal of (5) resembles a periodic signal and the discrete components dominate the low frequencies. On the other hand, if the $m(kT_s)$ values are large, then the

PPM signal looses its resemblance with a periodic signal and the continuous component dominates the low frequency range of the spectrum as well as the high frequency range.

Finally, as in the previous analyzed cases the term $|P(f)|^2$ shapes the overall spectrum and limits bandwidth occupation to finite values.

When the different $m(kT_s)$ are not independent it is possible to derive a generalized expression for the PSD which can be expressed as follows:

$$\mathbf{P}_{x_{PPM}}(f) = \frac{|P(f)|^2}{T_s} \sum_{n=-\infty}^{+\infty} \left\langle e^{-j2\pi f(m(l+n)T_s - m(l))} \right\rangle e^{-j2\pi f n T_s}. \quad (13)$$

B.2 The PPM-TH-UWB case

We can now refer back to the PPM-TH-UWB signal as expressed by (2) and establish a relationship with the PPM signal of (5), i.e., between $m(kT_s)$ and the θ time dither process which incorporates the time-shifts η and ϵ introduced by the time-hopping code and the PPM modulator.

Since ϵ is much smaller than η, θ is quasi-periodic and follows closely the periodicity of the time-hopping code. We can reasonably in a first approximation make the hypothesis that the effect of the ϵ shift on the PSD is not significant with respect to η. In this case the modulating signal in (2) is periodic and the resulting PSD follows (10), that is, the PSD is discrete and contains discrete frequency components located at the fundamental and pulse repetition frequencies and their harmonics, and at linear combinations of the above. The modulating periodic waveform has here period $T_p = N_p T_s$ and fundamental frequency $f_p = 1/T_p$. Note that pulse repetition frequency $1/T_s = N_p/T_p$ is a multiple of f_p, and therefore the PSD is composed of lines occurring at $1/T_p$ and harmonics.

The case $N_p = 1$ corresponds to the actual absence of coding and generates a PSD composed of lines at $1/T_s$ and harmonics. Power concentrates on spectrum lines with the undesirable effect of spectral line peaks. This is not a surprise since having neglected the effect of ϵ, the signal of (2) is a periodic train of pulses occurring at multiples of T_s.

If as common practice N_p is set equal to N_s, i.e., the periodicity of the code coincides with the number of pulses which represent a single bit, spectrum lines occur at $1/T_b$ and harmonics, where $T_b = N_s T_s = N_p T_s$ is the bit interval. Although the spectrum is still discrete, spectrum lines occur at frequencies which are much more numerous than in the previous case for equal bandwidth, since $1/T_b < 1/T_s$. The whitening effect of the code is visible in that power distributes over a larger number of spectrum lines, and spectral peaks are less accentuated.

When we make N_p larger than N_s the above effect is more prominent, and if N_p is not a multiple of N_s several spectral lines generated by linear combination of $1/T_p$ and $1/T_s$ fill up the power spectrum with a beneficial smoothing effect.

The extreme case $N_p \to \infty$ corresponds to a lack of periodicity in the signal of (2). In this case the time dither process can be assimilated by the random modulating signal $m(kT_s)$ and its power spectrum is given by (11). All observations made about (11) are valid here, i.e., the spectrum has two components, one continuous and one discrete. The discrete term corresponds to a periodic component of the signal which reduces with increasing variance in the position of the pulses. Also note that in the present case the time-hopping code generates time shifts which span the entire T_s interval. Therefore the values cannot be considered as small, and we can expect a reduction of the periodic component in the signal, i.e., of the discrete component in the spectrum.

In the presence of many such signals, i.e., in a multi-user environment, we can expect that the aggregate signal shows little periodicity, and the comments corresponding to the random modulating case apply.

The case of a system composed of a few users using the same value for N_p should be considered as of a periodic type, with the resulting cumulative signal having a discrete spectrum, if all users were synchronized. However, note that under the realistic hypothesis of asynchronous users we can expect that for several users, the multi-user signal looses its periodicity and its spectrum is well represented by (11).

A more refined analysis requires relaxing the hypothesis of an inconsequential effect of the PPM time shift ϵ. A straightforward solution to this problem, corresponding to the common case $N_p = N_s$, is to consider (2) in which first the effect of is neglected, i.e., one defines a signal $v(t)$ given as:

$$v(t) = \sum_{j=1}^{N_s} p(t - jT_s - \eta_j). \quad (14)$$

The Fourier transform of the above signal is:

$$P_v(f) = P(f) \sum_{m=1}^{N_s} e^{-j2\pi f(mT_s + \eta_m)}. \quad (15)$$

If one considers now $v(t)$ as the basic multi-pulse used for transmission and apply the ϵ PPM shift one obtains the following expression for the transmitted signal:

$$s(t) = \sum_{j=-\infty}^{+\infty} v(t - jT_b - \epsilon \cdot b_j), \quad (16)$$

which is a PPM modulated waveform in which now the shift is ruled by the sequence of data symbols **b** emitted by the source. Note that the repetition code is now incorporated into the multipulse. If we can assume **b** to be a stationary discrete random process, and the different extracted random variables b_k to be statistically independent with a common probability density function $w(\mathbf{b})$, then the signal of (16) has PSD as of (11) in which the Fourier Transform of the pulse waveform $P(f)$ is given by (15). Given that the multi-pulse repetition rate is T_b, one has thus:

$$\mathbf{P}_s(f) = \frac{|P_v(f)|^2}{T_b} \left[1 - |W(f)|^2 + \frac{|W(f)|^2}{T_b} \sum_{n=-\infty}^{+\infty} \delta(f - \frac{n}{T_b}) \right]. \quad (17)$$

Equation (17) shows the double effect of the time hopping code through $P_v(f)$, and of the time-shift introduced by the PPM modulator, the characteristics of which follow the statistical properties of the source. Note that the discrete component of the spectrum has lines at $1/T_b$. The amplitude of the lines is

modulated by the statistical properties of the source represented by $|W(f)|^2$. If p indicates the probability of emitting a 0-bit (no shift) and $(1-p)$ the probability of emitting a 1-bit (ϵ shift) one can write:

$$|W(f)|^2 = 1+2p^2(1-cos(2\pi f\epsilon)-2p(1-cos(2\pi f\epsilon))). \quad (18)$$

If the source emits equiprobable symbols 0 and 1 then (18) simplifies into $|W(f)|^2 = \frac{1}{2}(1+cos(2\pi f\epsilon))$. Here the time shift is small and therefore the discrete components dominate the spectrum. Assuming, simplistically, that ϵ is negligible, (17) is periodic with period $1/T_b$.

Note that (17) can be applied to any type of source, not necessarily binary.

C. Power Spectral Density of BAM Modulated Time-Hopping UWB Signals

Consider a sequence **a** composed of ± 1 values ($a_k = 2b_k - 1$, $-\infty < k < +\infty$) which amplitude modulates the time-hopped train of pulses. The generated signal can be expressed as in (3) in the specific case of transmission of $p(t)$ for $a_k = 1$ and of $-p(t)$ for $a_k = -1$. By applying the same procedure as in the previous paragraph, consider now the common case of $N_p = N_s$ and the basic multi-pulse waveform $v(t)$ as in (14) which is amplitude modulated by the source emitting **b** sequence after transformation in a 1 sequence. (3) can be rewritten as:

$$s(t) = \sum_{j=-\infty}^{+\infty} b_j v(t - jT_b). \quad (19)$$

Equation (19) is a straightforward BAM waveform with basic multi-pulse $v(t)$ having the Fourier transform given by (16). For this type of waveform the PSD can be easily derived (Proakis, 1995) as described in the following paragraph.

D. Spectral Density of Direct-Sequence UWB Signals

The PSD of a DS-UWB signal is more easily derived than the TH-UWB case since pulses occur here at multiples of T_s.

It is well known (see for example Proakis, 1995) that signal in (4) is not wide-sense stationary but can be made such by introducing a random phase epoch Θ, uniformly distributed over $[0,\ T_s]$ and independent of **d**. The DS-UWB random process modifies in:

$$s(t+\Theta) = \sum_{j=-\infty}^{+\infty} d_j p(t - jT_s + \Theta). \quad (20)$$

The PSD of (20) can be determined in a straightforward manner by computing the autocorrelation function of $s(t)$, and then its Fourier transform. One obtains:

$$\begin{aligned} \mathbf{P}_{xDS}(f) &= \frac{|P(f)|^2}{T_s} \sum_{m=-\infty}^{+\infty} R_d(m) e^{-j2\pi f m T_s} \\ &= \frac{|P(f)|^2}{T_s} \cdot P_c(f), \end{aligned} \quad (21)$$

where $P_c(f)$ is the so-called code spectrum and is the discrete-time Fourier transform of the autocorrelation function of **d**, $R_d(m)$. Since $R_d(m)$ is an even function one has:

$$\begin{aligned} P_c(f) &= \sum_{m=-\infty}^{+\infty} R_d(m) e^{-j2\pi f m T_s} \\ &= R_d(0) + 2 \sum_{m=-\infty}^{+\infty} R_d(m) cos 2\pi f m T_s. \end{aligned} \quad (22)$$

Equation (21) shows that the spectrum of the DS-UWB signal is governed by two terms: the transfer function of the pulse shaping filter $P(f)$, as for TH-UWB signals, and the code spectrum $P_c(f)$. Note that if the sequence **d** were composed of independent symbols $R_d(m)$ would be different from 0 only for $m = 0$ and therefore $P_c(f)$ would be independent of f. In this case the spectrum of the DS signal would be entirely governed by the properties of $p(t)$.

III. POWER LIMITS AND PULSE SHAPING

A. Power Limits

UWB radio signals potentially overlap with other signals in the frequency domain. Possible interference from and onto other communication systems must be contained within regulated values which indicate the maximum tolerable power to be present "in the air" at any given frequency, as set by emission masks. The limitation is on the effective radiated power, i.e., the effective isotropic radiated power (EIRP) given by the product of the available power of the transmitter P_{TX}, that is the maximum power that the transmitter can transfer to the transmit antenna, and the gain of the antenna at the transmitter G_{AT}. In some cases reference is made to the field strength V in place of available power, i.e., the voltage that one should apply to the free-space impedance Z_{FS} in order to obtain P_{TX}. Z_{FS} is related to permeability and permittivity of free space and is about 377 ohms (the exact value being 120π). In principle Z_{FS} is independent of frequency. The relation between field strength (expressed in volts) and available power (expressed in watts) is $P_{TX} \simeq \frac{V^2}{377}$. This power is an average power. Given the energy of a single pulse E_p, and $N_s E_p$ the total energy of the pulses representing one bit, the average power is computed by averaging over the bit interval T_b, and is thus:

$$P_{av} = \frac{N_s E_p}{T_b} = \frac{N_s E_p}{N_s T_s} = \frac{E_p}{T_s}. \quad (23)$$

Equation (23) indicates that different signals may have same P_{av} with tremendous difference in pulse energy E_p, depending on pulse repetition rate. At equal average power, signals with low repetition rate present higher E_p. For equal pulse duration this is equivalent to say that the maximum instantaneous power may be significantly different among signals with similar average power.

Currently available UWB emission masks for indoor communications as issued by the FCC (FCC, 2002) limit the operation to a -10 dB bandwidth lying between 3.1 and 10.6 GHz, and sets very stringent limits on out of band emission masks. The average power values are set as shown in Fig. 3 The rule also specifies a limit on the peak level of emission within a 50MHz

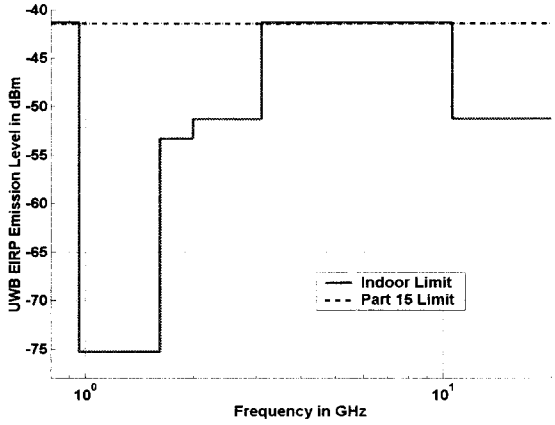

Fig. 3. FCC indoor emission mask for UWB devices (FCC, 2002).

bandwidth centred on the frequency f_M at which the highest radiated emission occurs. The limit is set to 0 dBm/50MHz, which is the average power computed over a frequency range of 50 MHz around f_M is limited to 0 dBm.

B. Pulse Shaping

Pulse shaping is crucial since as shown in Section II it affects the PSD of the transmitted signal.

Although often called monocycle, the adopted pulse in UWB communication systems is rarely a cycle of a sinusoidal wave. It is in fact less difficult and less expensive to generate nonsinusoidal pulses than pulse modulated sinusoidal waves. Generating pulses of duration on the order of the nanosecond with an inexpensive technology (CMOS chips) has become possible after UWB large current radiator (LCR) antennas were introduced by Harmuth (1990). The LCR antenna is driven by a current and the antenna radiates a power which is proportional to the square of the derivative of current. When a step-function current for example is applied to the antenna a pulse is generated. The steeper the step-function current, the narrower the generated pulse. The pulse shape which can be generated in the easiest way by a pulse generator has actually a bell shape such as a Gaussian, as shown in Fig. 4 and one can write $p(t) = \pm\frac{1}{\sqrt{2\pi\sigma^2}}e^{(\frac{t}{2\sigma^2})} = \pm\frac{\sqrt{2}}{\alpha}e^{-\frac{2\pi t^2}{\alpha^2}}$. In order to be radiated in an efficient way, a fundamental characteristic of the pulse is to have a zero dc offset. Several pulse waveforms might be considered provided that this condition is verified. Gaussian derivatives are suitable. Actually, the most commonly adopted pulse shape is modelled as the second derivative of a Gaussian function (Win and Scholtz, 2000). This pulse is usually referred to as the pulse at the receiver, i.e., after passing through the transmitter and receiver antennas. Other pulse shapes have also been proposed such as the Laplacian (Conroy *et al.*, 1999), compositions of Gaussian pulses having same length and reversed amplitudes with a fixed time gap between the pulses (Hämäläinen *et al.*, 2001), or Hermite pulses (Ghavami *et al.*, 2002).

Ideally a second derivative Gaussian pulse can be obtained at the output of the transmit antenna if the antenna is fed with a current pulse shaped as the first derivative of a Gaussian (and

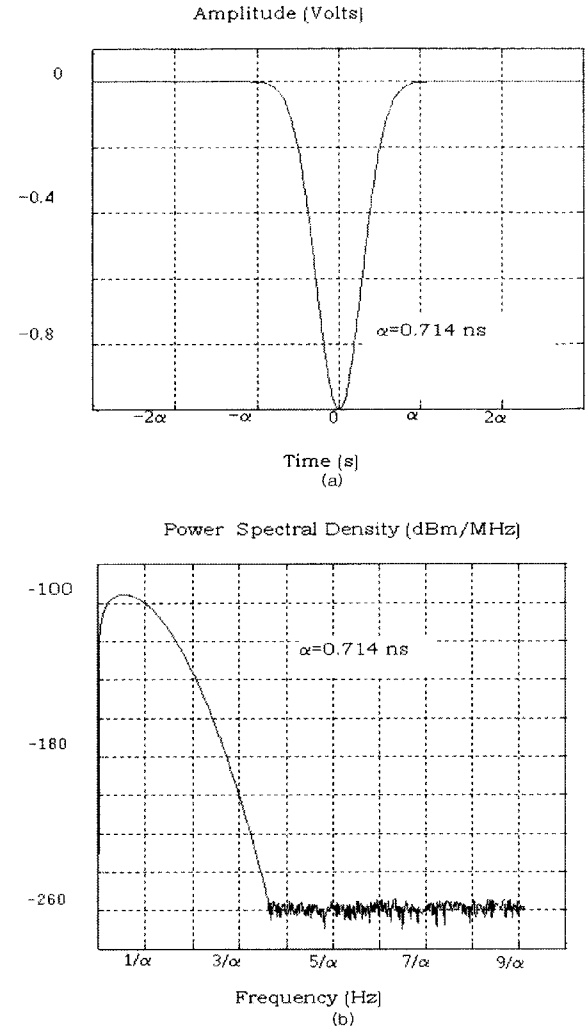

Fig. 4. Example of a Gaussian pulse $p(t) = \pm\frac{1}{\sqrt{2\pi\sigma^2}}e^{-\frac{t}{2\sigma^2}} = \pm\frac{\sqrt{2}}{\alpha}e^{-\frac{2\pi t^2}{\alpha^2}}$: (a) Waveform, (b) corresponding PSD.

thus zero dc current), the radiating pulse being proportional to the derivative of the drive current in an ideal antenna.

Shaping the spectrum by changing the pulse waveform is an interesting feature of impulse radio. Basically the spectrum may be shaped in three different ways: pulse width variation, pulse derivation, and combination of base functions.

Consider the Gaussian pulse as a case study. Pulse width can be reduced by reducing α , and by doing so the bandwidth of the transmitted signal is enlarged. This effect is shown in Fig. 5 on both waveform and PSD.

The peak frequency of the pulse is increased with increasing derivation order. This is shown in Fig. 6 for the first 20 derivatives of the Gaussian pulse. It is possible to find a general relationship between the peak frequency f_{peak}, the order of derivation k and the shape factor α, by observing that the Fourier transform of the k-th derivative has the property: $X_k^{'}(f) \propto f^k \cdot e^{-\frac{\pi \cdot f^2 \cdot \tau_m^2}{2}}$ which leads to a peak frequency for the k-th derivative $f_{peak} = \sqrt{k} \cdot 1/\alpha\sqrt{k}$. The behavior of the peak frequency as a function of for the first 20 derivatives of the

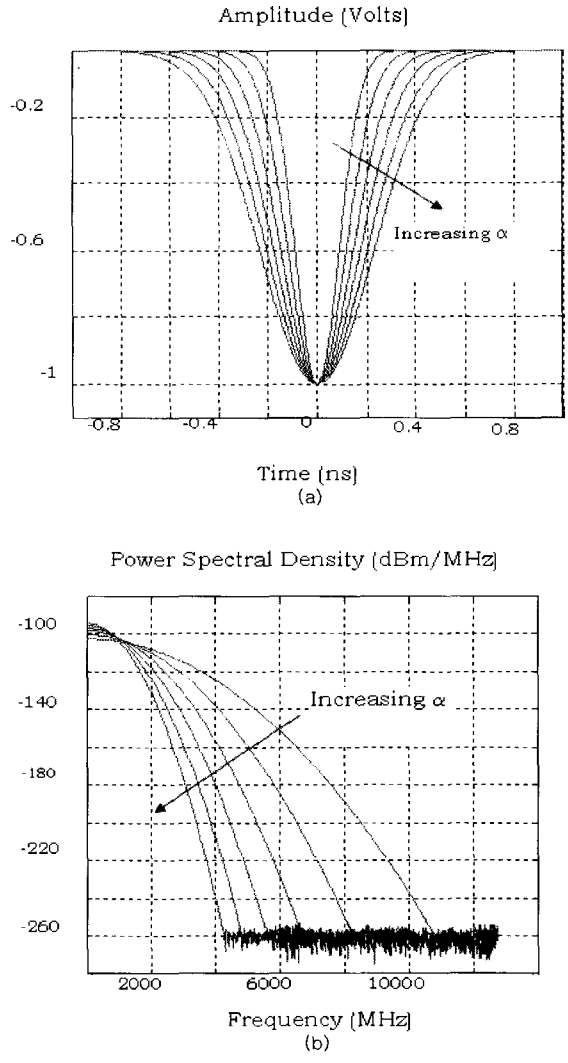

Fig. 5. The Gaussian pulse case: Effect of α (a) pulse duration and (b) PSD.

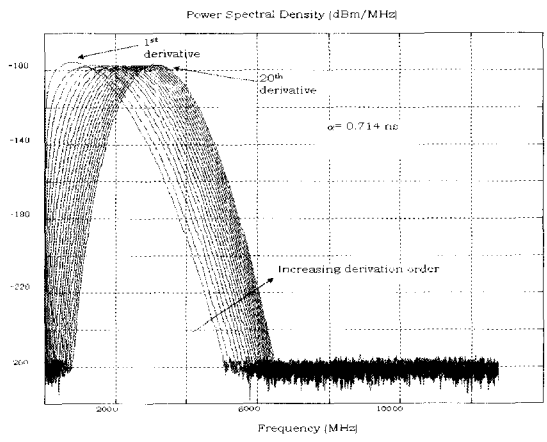

Fig. 6. PSD of the first 20 derivatives of the Gaussian pulse.

Gaussian pulse is presented in Fig. 7. Regarding the bandwidth, Fig. 8 shows the variation of the -10 dB bandwidth for the set of 20 derivatives of the Gaussian pulse.

Shaping the spectrum with a single waveform is usually not sufficient to fulfil requirements. Higher flexibility may be achieved by using several base waveforms in order to produce the desired pulse shape, for example by a linear combination of them. One can apply standard procedures for error minimization such as the least-square-error (LSE). Fig. 9 shows the result obtained by linearly combining the first 20 derivatives of the Gaussian pulse in order to fit the FCC mask, using the LSE method.

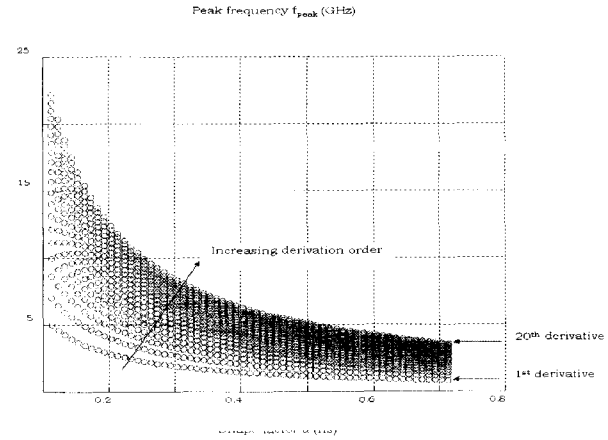

Fig. 7. Variation of peak frequency with α for the first twenty derivatives of the Gaussian pulse.

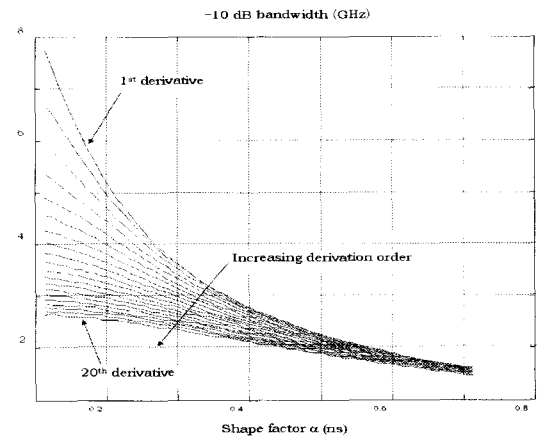

Fig. 8. Variation of -10 dB bandwidth with α for the first twenty derivatives of the Gaussian pulse.

IV. MULTIPLE ACCESS

A. Multiple Access Capacity

The power spectral density limit defined by the FCC mask, or similar regulations in other parts of the world, is the primary driver affecting the multiple access capacity of UWB communications networks. As a regulatory constraint, this power spectral density limitation may change in the future so as to increase or reduce the amount of allowed transmit power. Any further modifications of rules governing the use of the wide radio frequency spectrum intended for UWB communications will be impacted with the success and penetration of deployed UWB technology and its impact on society, as well as the reassessment of potential

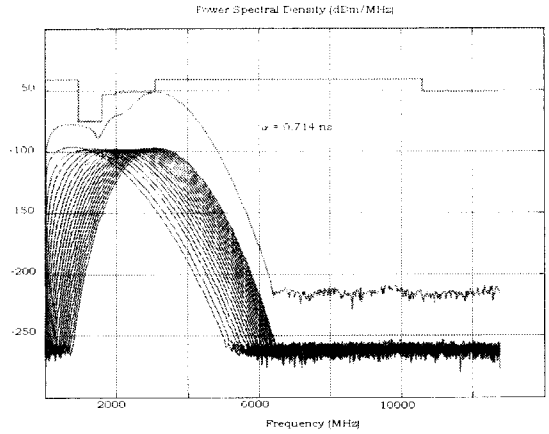

Fig. 9. PSD of the base functions (solid plots) and of the combined waveform (dashed plot) vs. FCC mask (FCC, 2002).

incremental interference on services in affected radio frequency bands. Any speculation as to how this process might evolve is beyond the scope of this paper. Though, it is important to understand that the regulatory limits should also be a reflection of what is achievable with present and future technology, not just which technology active industrial players deployed or are planning to deploy. This argument should be applicable to both UWB communication systems as well as systems impacted by UWB interference. However, it is clear that regulatory limits will exist, because of the nature of spectrum sharing, and whatever form these limits may take they will impact the capacity of UWB communication systems.

In addition to regulatory factors, the capacity of UWB systems is affected by physical phenomena such as path loss and multipath channel characteristics. The path loss at shorter distances (5 to 10 meters) appears to be closer to the free-space path loss. All experimental evidence suggests very rich multipath structure, which for very high date rates may result in multipath spreads being longer than several symbol intervals. In addition to affecting the capacity, the latter may also impact practical receiver realizations, imposing the receiver processing structures or techniques such as RAKE or equalization.

While the regulatory and physical constraints ultimately determine the theoretical capacity of UWB systems, the communications capacity may also be impacted by design constraints, such as the choice of forward error correction coding and modulation, the choice of hardware components or network topology, and medium access control protocols.

To facilitate the analysis and discussion of multiple access capacity, let us first define system parameters that define the operational scenario. A set of assumptions for a representative link budget analysis is shown in Table 1.

The last assumption in Table 1 suggests that we imply a spread spectrum system of some form will be considered. One can argue about the choice for total system losses of 7dB, but most practical systems should be able to achieve this, give or take a couple of dBs. The assumption of no multipath is very simplifying, but it enables us to quantitatively compare different approaches without going into elaborate analysis and simulations.

Table 1. System assumptions for multiple access capacity analysis.

Effective system bandwidth	7.5GHz
Signal PSD limit	-41.3dBm/MHz
Noise PSD	-174dBm/Hz
Path loss with distance	$\sim d^2$
Path loss at 1m	44dB
Multipath	No
Total system losses	7dB
Processing gain (spreading factor)	20

To illustrate the capacity potential of a UWB system with attributes shown in Table 1, we assume DS CDMA and use results for spectral efficiency with random spreading. These results are asymptotic in $K(K \to \infty)$, where K represents the number of active users, but for the fixed ratio $\beta = K/N$, where N represents the spreading factor. For the single user matched filter receiver the spectral efficiency in bits/chip, from (Verdu and Shamai, 1999), is given by

$$\lim_{K\to\infty} C^{mf} = \frac{\beta}{2} log\left(1 + \frac{SNR}{1+\beta SNR}\right), \tag{24}$$

where $SNR = 2rE_b/N_0$ represents the signal-to-noise ratio per coded symbol. The optimum spectral efficiency is given by (Verdu and Shamai, 1999) as

$$\begin{aligned}\lim_{K\to\infty} C^{mf} &= \frac{\beta}{2} log\left(1 + SNR - \frac{1}{4}F(SNR,\beta)\right) \\ &+ \frac{1}{2} log\left(1 + SNR - \frac{1}{4}F(SNR,\beta)\right) \\ &- \frac{log\, e}{8SNR}F(SNR,\beta),\end{aligned} \tag{25}$$

where $F(x,z) = \left(\sqrt{x(1+\sqrt{z})^2+1} - \sqrt{x(1-\sqrt{z})^2+1}^{\,2}\right)$. We will use these formulas for moderate values of K and N. It was previously shown by simulation that asymptotic multiuser capacity results are a good approximation at moderate values of processing gains and numbers of users (Vojcic, 1997).

In Fig. 10 we compare the optimum sum capacity with those for the single user and 10 users with perfect power control and single-user matched filter detection. In all cases, the spreading factor of 20 and other parameters from Table 1 are assumed. For the single user case we used the standard Shannon capacity formula. To obtain the sum capacity from spectral efficiency, we assumed that the bandwidth is reciprocal of chip rate and multiplied the spectral efficiency with the total available bandwidth.

The single user case is representative of scenarios where only one spread spectrum transmission is present at any given time and multiple access is achieved by a time-sharing between users. That is similar to IEEE 802.15.3, except that we assume a "genie" that assigns the channel use without any overhead or capacity loss. One message from this figure that contradicts the practice in 802.15.3 is that to improve the sum capacity one would like to have multiple simultaneous transmissions. It can be seen that a manifold increase in capacity can result. We will discuss later what kind of topology or network organization might be suitable to achieve that goal. Another message is that advanced multiuser detection/decoding may enable a manifold improvement in the sum capacity compared to the single-user matched

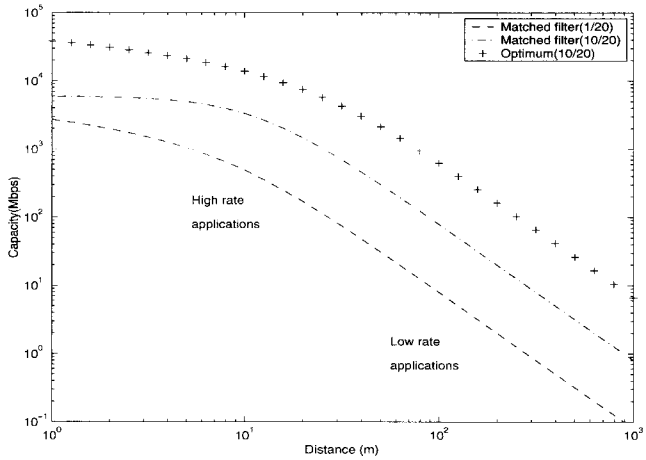

Fig. 10. Capacity of DS CDMA with matched filter and optimum detection.

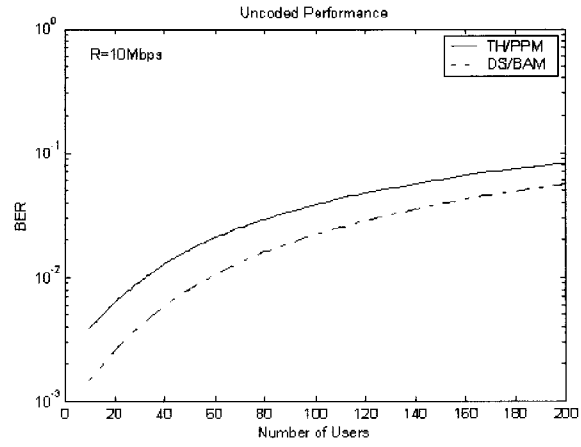

Fig. 11. Uncoded BER performance of multiple access with DS/BAM and TH/PPM.

filter detection, for the assumed range of operational parameters. Although at very high data rates such signal processing may not be inexpensive to achieve at the present time, it certainly provides an upper bound on the capacity that might be attainable in the future. Although we used the capacity results for DS CDMA we believe that similar conclusions can be drawn for other CDMA schemes, such as TH, for example.

B. TH CDMA versus DS CDMA

TH CDMA with PPM dominated initial directions in the development of impulse radio based UWB communications (Scholtz, 1993; Win and Scholtz, 2000), while DS CDMA was gaining more proponents in recent years (Huang and Li, 2001; Foerster, 2002; Vojcic and Pickholtz, 2003). Other approaches are possible as well, including FDMA, TDMA and hybrid combinations of TDMA or FDMA with CDMA schemes. Here we will briefly review a comparison of TH/PPM CDMA and DC CDMA employing binary antipodal modulation (BAM), i.e., "0" and "1" signaling waveforms having opposite polarity. For the former we will use results from (Scholtz, 1993). It was shown in (Vojcic and Pickholtz, 2003) that the signal-to-noise plus interference ratio (SNIR) for the i-th user in a K-user DS CDMA system with BAM and arbitrary chip shape can be expressed as

$$SNIR_i = \left[\frac{N_0}{2E_i} + \frac{\xi}{NE_i} \sum_{k \neq i}^{K} E_k \right]^{-1}, \qquad (26)$$

where ξ depends on the choice of pulse shape and is given by $\xi = \frac{1}{T_c} \int_0^{T_c} (\hat{R}_p^2(\psi) + R_p^2(\psi)) d\psi$, $\hat{R}_p(\psi) = \int_{\Psi}^{T_c} p(t)p(t-\psi)dt$, $R_p(\psi) = \hat{R}_p(T_c - \psi)$. By making the usual Gaussian assumption for multiple access interference, which is reasonably accurate for $K, N >> 1$, one can simply use the SNIR formula from (26) to approximate the result for probability of bit error

$$P_i = Q\left(\sqrt{SNIR_i}\right). \qquad (27)$$

In Fig. 11 we compare TH/PPM and DS/BAM CDMA for data rate R=10Mbps and pulse shape and all other system parameters as in (Scholtz, 1993). Specifically, the pulse shape is defined by

$$p(t) = \left[1 - 4\pi\left(\frac{t - t_d}{\lambda}\right)^2\right] \exp\left[-2\pi\left(\frac{t - t_d}{\lambda}\right)^2\right],$$

where t_d=0.35ns and λ= 0.2877, which results in pulse duration of 0.7ns. In addition, the time displacement of "0" and "1" pulses is ϵ=0.156 ns, resulting in optimum cross-correlation of PPM signaling waveforms of ρ=-0.6183. It is assumed that $E_i/N_0 = 10dB$. For simplicity, in both cases we assume no multipath.

As can be seen from Fig. 11, DS/BAM outperforms TH/PPM because of more efficient modulation constellation. Even optimized PPM with ρ=-0.6183 is inferior in squared distance of signal points relative to BAM by 0.92dB. In addition, the pulse displacement of ϵ=0.156 ns in optimized PPM results in a reduction in processing gain relative to DS/BAM with the factor (0.7+0.156)/0.7=0.87dB. It should be noticed that orthogonal PPM would result in an additional loss in performance relative to DS/BAM. A probability of error comparison for coded TH and DS CDMA systems is also shown in (Vojcic and Pickholtz, 2003). Another potential advantage of DS CDMA with BAM is a better peak-to-average power ratio, which is relevant to both regulatory aspects and hardware implementation.

C. Network Topology and Multiple Access

It appears that many ongoing developments of UWB systems concentrate heavily or exclusively on the physical layer, without significant considerations being given to network topology, medium access control and, perhaps, even network layer. This incurs the risk of missing the opportunity for cross-layer optimization, and possibly leading to suboptimum system designs. A possible approach for modeling and optimizing UWB network design was proposed in (Baldi,De Nardis,and Di Benedetto, 2002). The proposed methodology defines a global network cost function which takes into account both physical and network layers parameters. The network cost function is

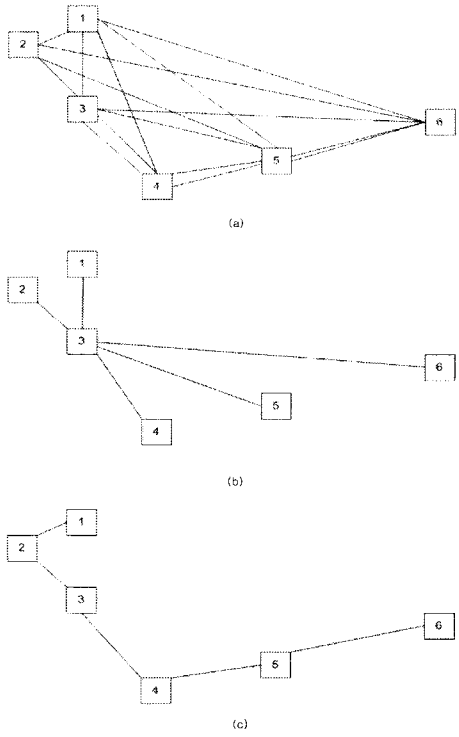

Fig. 12. Different network topologies for UWB systems : (a)Peer to peer topology, (b)star topology, (c)multi-hop topology.

then used to determine best routes, and drive the network to a desired topology of active links.

In this subsection we will discuss some topological aspects of network design and how they relate to the previously discussed capacity results as well as other practical considerations of the multiple access approach.

One of the most mentioned network topologies in the context of UWB communications systems is the single hop peer-to-peer topology. One example of such a topology is shown in Fig. 12(a) The main advantage of such an approach is that each destination is reached in one hop, minimizing the delay and number of transmissions per information packet. However, one of the main disadvantages of this approach is that the throughput in such a topology is limited by the maximum distance between two peer nodes. Even more importantly, the single hop peer-to-peer topology is not suitable for multiple simultaneous transmissions per network. As we indicated in Section III.A, multiple simultaneous CDMA transmissions would lead to a higher capacity. The reason that multiple simultaneous transmissions may not be a viable approach for this topology is the near-far problem that may result from simultaneous transmissions with a spontaneous CDMA. On the other hand, scheduling multiple transmissions and assigning the transmit power levels such that the near-far effect is minimized may be extremely complicated. One solution would be to employ multiuser detection that can effectively combat the near-far problem and maximize communication capacity. Though, this may not be a viable approach in the near future because it is desired to minimize receiver complexity, in order to keep the cost of UWB devices low. These considerations probably led to the time-sharing approach, which is characterized by only one transmission per network at any given time, such as in IEEE 802.15.3. Essentially, CDMA would only be used to reduce inter-network interference, when adjacent networks exist in relative proximity.

The disadvantages of peer-to-peer topology could be overcome by introducing a star topology, similarly as in cellular networks. An example of such a network is shown in Fig. 12(b). In this case one node is chosen as the master, or base station and all transmissions go through it. In general, it is now required to have two hops to reach the destination, unless the master station is the destination. This might appear as an inefficient approach, at first glance, because two transmissions are required per information packet. However, this enables multiple simultaneous transmissions per network. The near-far problem is easily avoided by means of power control. In addition, by conveniently choosing the master station to be centrally located in the topology, the range, or throughput, of the network can be maximized. Moreover, since multiple simultaneous transmissions are possible, the peak data rate per source-destination pair can be reduced, which can be exploited to further increase the range. Since the PSD limit is assumed per station (node), it should be clear that the throughput per slot might be different in the two different directions, forward (master station to other stations) and reverse (other stations to master station). For example, in the scenario of Fig. 12(b) for the reverse link, possibly all five transmissions (from nodes 1, 2, 4, 5, and 6) might be possible simultaneously. However, on the forward link the number of simultaneous transmissions would be limited jointly by the PSD limit and individual rate requirements. In addition, if in the forward link power control is employed, the distances of individual stations, (i.e., their path losses) would also affect the number of simultaneous transmissions. The main disadvantage of this approach is the increased complexity of the master station that now must be able to receive multiple packets simultaneously. This may be a small price to pay for increased range and/or capacity which may make UWB more competitive for local area network (LAN) applications. Though, the star technology, because of the PSD limit, may still be insufficient to meet the range requirements of LANs.

In Fig. 12(c), a multi-hop topology is shown which also provides the potential for multiple simultaneous transmissions but in this case not to/from single master station. In this case the multiple transmissions are over spatially separated links and to different destinations. For example in one packet interval we may have simultaneous transmissions 1–2, 3–4 and 5–6, while in the next packet interval transmissions 2–3 and 4–5 would be possible, without causing the near-far problem. The routing and scheduling can be designed such that any station receives only one packet at any given time. The main advantage of this topology is that it can be tailored to architectural needs of network deployment and that it can achieve much longer ranges than in the case of the previous two configurations. The disadvantages are that multiple transmissions over the channel may be needed for a single information packet and that the network layer protocols in this case would have additional complexity. The former may be more than compensated for by reduced hop length which would enable higher throughput per link. For example, by reducing the longest hop by the factor 3 in this case, relative to the peer-to-

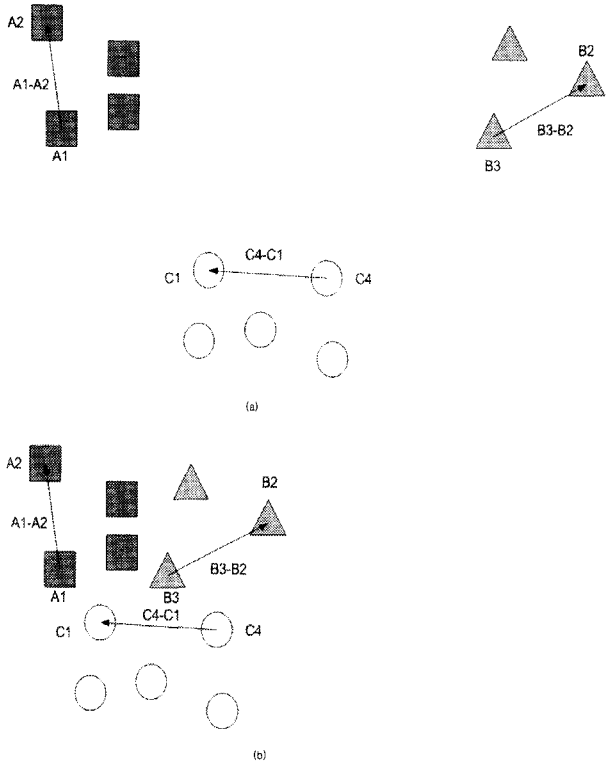

Fig. 13. Examples of inter-network interference scenarios : (a)Spatially separated adjacent network, (b)closely spaced adjacent network.

peer topology, a power gain of $3^2 = 9$ is achieved which can be utilized to improve spectral efficiency by transmitting more bits per channel symbol. Considering all advantages and disadvantages, this topology represents a promising approach to enable UWB radio to become competitive for LAN applications.

D. Inter-network Interference

In many operational situations there might be adjacent UWB networks causing inter-network interference. In Fig. 13 we show two such scenarios: a) when adjacent networks are widely separated and cause no significant inter-network interference and b) when the adjacent networks are very close and cause a significant amount of mutual interference. In the first case it is relatively simple to deal with the processing gain of employed spread spectrum system. On the other hand, in the case shown in Fig. 13b, transmissions A1-A2 and B3-B2 may cause excessive interference, i.e., the near-far problem, to node C1 of link C4-C1. This is a consequence of the fact that in this case the distance between C4 and C1 is larger than the distance between A1 and C1 or the distance between B3 and C1.

This kind of near-far problem is harder to deal with multiuser detection than the case of intra-network interference discussed earlier, because adjacent networks are not coordinated or synchronized. However, there are blind interference cancellation schemes that may efficiently combat this kind of interference. Though, the argument that UWB radios need as simple processing as possible is still applicable and may rule out application of these advanced multiuser signal processing techniques until some time in the future.

As mentioned in Section I, another approach, currently under consideration for IEEE 802.15.3, is to have multiple non-overlapped narrower band UWB waveforms, whereby multiple bands could be concatenated to achieve full capacity (Foerster, Somayazulu and Roy 2003). This multi-band approach enables frequency division between adjacent networks exposed to the near-far effect. Additional potential advantage of the multiband approach is a relatively simple co-existence with non-UWB narrowband services. Though, this problem can also be dealt efficiently with notch filtering. An alternative approach to combat near-far problem between adjacent networks would be to employ time division between adjacent networks and each network would employ full bandwidth for maximum multipath resolution. This approach assumes that some degree of synchronization (propagation of time reference) between adjacent networks is necessary.

REFERENCES

[1] P. Baldi, L. De Nardis, and M. G. Di Benedetto, "Modelling and optimization of UWB communication networks through a flexible cost," *IEEE JSAC Special Issue on UWB Radio in MultiAccess Wireless Communications*, pp. 1733–1744, 2002.

[2] W. R. Bennett, "New results in the calculation of modulation products," *Bell System Tech. J.*, pp. 228–243, 1933.

[3] W. R. Bennett, "Response of a linear rectifier to signal and noise," *J. Acoust. Soc. Am.*, pp. 164–172, 1944.

[4] W. R. Bennett, "The biased ideal rectifier," *Bell System Tech. J.*, pp. 139–169, 1947.

[5] J. T. Conroy, J. L. LoCicero, and D. R. Ucci, "Communication techniques using monopulse waveforms," in *Proc. MILCOM'99*, vol. 2, pp. 1181–1185.

[6] DARPA, OSD/DARPA, *Assessment of Ultra-Wideband (UWB) Technologies*, Ultra-Wideband Radar Review panel.

[7] FCC, "revision of part 15 of the commission's rules regarding ultra-wideband transmission systems," *Federal Communications Commission, ET Docket.* pp. 98–153, 2002.

[8] J. R. Foerster, "The performance of a direct-sequence spread ultra-wideband system in the presence of multipath, narrowband interference, and multiuser interference," in *Proc. IEEE Ultra Wideband Systems and Technologies*, May 20–23, 2002, pp. 87–91.

[9] J. R. Foester, V. Somayazulu, and S. Roy, "A multi-banded system architecture for ultra-wideband communications," in *Proc. MILCOM'2003*, Oct. 13–16, 2003, pp. 903–908.

[10] M. Ghavami *et al.*, "A novel UWB pulse shape modulation system," Wireless Personal Communications , pp. 105–120, 2002.

[11] I. Guvenc and H. Arslan, "On the modulation options for UWB systems considering the overall system aspects," in *Proc. MILCOM'2003*, Oct. 13–16, 2003, pp. 892–897.

[12] M. Hämäläinen *et al.*, "In-band interference power caused by different kinds of UWB signals at UMTS/WCDMA frequency bands," in *Proc. RAWCON'2001*, Aug 19–22, 2001, pp. 97–100.

[13] H. F. Harmuth, *Radiation of Nonsinusoidal Electromagnetic Waves*, Academic Press, New York.

[14] X. Huang and Y. Li, "Generating near-white ultra-wideband signals with period extended PN sequences," in *Proc. VTC'2001*, May 6–9, 2001.

[15] M. S. Iacobucci and M. G. Di Benedetto, "Multiple access design for impulse radio communication systems ," in *Proc. ICC'2002*, vol. 2, 2002, pp. 817–820.

[16] D. C. Laney *et al.*, "Multiple access for UWB impulse radio with pseudochaotic time hopping," *IEEE J. Select. Areas Commun.*, vol. 20, no. 9, 2002, pp. 1692–1700.

[17] J. G. Proakis, *Digital Communications*, McGraw-Hill Inc.

[18] J. G. Proakis and M. Salehi, *Communication Systems Engineering*, Prentice-Hall International, Inc.

[19] H. E. Rowe, *Signals and Noise in Communications Systems*, D. Van Nostrand Company, Inc, 1965.

[20] R. A. Scholtz, "Multiple access with time-hopping impulse modulation," in *Proc. MILCOM'93*, pp. 447–450.

[21] S. Verdu and S. Shamai, "Spectral efficiency of CDMA with random spreading," *IEEE Trans. Inform. Theory*, vol. 45, no. 2, pp. 622– 640, 1999.

[22] B. Vojcic, "Information theoretic aspects of multiuser detection," in *Proc. IRSS'97*, Mar. 1977.

[23] B. Vojcic and R. L. Pickholtz, "Direct-sequence code division multiple access for ultra-wide bandwidth impulse radio," in *Proc. MILCOM'2003*, Oct. 13–16, 2003, pp. 898–902.
[24] W. T. Webb and L. Hanzo, *Modern Quadrature Amplitude Modulation - Principles and Applications for Fixed and Wireless Channels*, IEEE Press and Pentech Press-London.
[25] M. Welborn, "System considerations for ultrawideband wireless networks," in *Proc. RAWCON'2001*, Aug. 2001.
[26] M. Z. Win and R. A. Scholtz, "Ultra-wide bandwidth time-hopping spread-spectrum impulse radio for wireless multiple-access communications," *IEEE Trans. Commun.*, vol. 48, no. 4.
[27] P. C. Yeh *et al.*, "Performance analysis of coded multi-carrier wideband systems over multipath fading channels," in *Proc. MILCOM'2003*, Oct. 13–16, 2003, pp. 909–914.

Maria-Gabriella Di Benedetto obtained her Ph.D. in Telecommunications in 1987 from the University of Rome La Sapienza, Italy. In 1991, she joined the Faculty of Engineering of University of Rome La Sapienza, where currently she is a Full Professor of Telecommunications at the Infocom Department. She has held visiting positions at the Massachusetts Institute of Technology, the University of California, Berkeley, and the University of Paris XI, France. In 1994, she received the Mac Kay Professorship award from the University of California, Berkeley. Her research interests include speech analysis and synthesis, and digital communication systems. From 1995 to 2000, she directed four European projects for the design of UMTS. Since 2000 she has been active in fostering the development of Ultra Wide Band (UWB) radio communications in Europe. She is currently the director for the Infocom Dept. of two European projects (whyless.com and UCAN) aimed at the design and implementation of UWB ad-hoc networks. Within the forthcoming 6th EU Framework her "Networking with UWB" research group will participate to the Pulsers Project which will integrate UWB research and development in Europe for the next years. Dr. Di Benedetto was co-editor for IEEE JSAC of a Special Issue on UWB Radio in Multi-Access Wireless Communications (December 2002).

Branimir R. Vojcic is a professor in, and Chairman of, the Department of Electrical and Computer Engineering at the George Washington University. He has received his D.Sc. degree from the University of Belgrade in Yugoslavia. His current research interests are in the areas of communication theory, performance evaluation and modeling mobile and wireless networks, code division multiple access, multiuser detection, adaptive antenna arrays, space-time coding and ad-hoc networks. He has also been an industry consultant and has published and lectured extensively in these areas. Dr. Vojcic is a Senior Member of IEEE, was an Associate Editor for IEEE Communications Letters.